Resonance Raman Spectrum of the Solvated Electron in Methanol: Simulation within a Cluster Model

Stefanie Neumann,[†] Wolfgang Eisfeld,[†] Andrzej L. Sobolewski,[‡] and Wolfgang Domcke*[,†]

Department of Chemistry, Technical University of Munich, D-85747 Garching, Germany, and Institute of Physics, Polish Academy of Sciences, PL-02668 Warsaw, Poland

Received: December 22, 2005; In Final Form: March 14, 2006

The microsolvation of the CH_3OH_2 hypervalent radical in methanol clusters has been investigated by density functional theory. It is shown that the CH_3OH_2 radical spontaneously decomposes within methanol clusters into protonated methanol and a localized solvated electron cloud. The geometric and electronic structures of these clusters as well as their vibrational frequencies have been characterized. Resonance Raman intensities, associated with the s → p transition of the unpaired electron, have been estimated for $CH_3OH_2M_n$ (M = CH_3OH, $n = 1-3$) clusters. It is shown that with increasing cluster size the simulated spectra converge toward the resonance Raman spectrum of the solvated electron in methanol measured recently by Tauber and Mathies (*J. Am. Chem. Soc.* **2004**, *126*, 3414). The results suggest that $CH_3OH_2M_n$ clusters are useful finite-size model systems for the computational investigation of the spectroscopic properties of the solvated electron in liquid methanol.

1. Introduction

The solvated electron is an important species throughout chemistry, physics, and biology. This applies not only to the solvated electron in water, the so-called hydrated electron, but also to the solvated electron in other solvents such as alcohols.[1−4]

The spectroscopic features of the solvated electron in different solvents, its EPR *g*-factors, and its chemical reactivity have been investigated extensively since the late 1950s to 1980s.[5−8] The optical absorption spectra of the solvated electron in different solvents consist of a single broad and asymmetric band. For the solvated electron in alcohols, this band is broader and more asymmetric than the absorption band of the hydrated electron.[9,10] In methanol, for example, the half width of the absorption band is 1.37 eV, compared with 0.85 eV in water. In methanol, the absorption maximum is located at 1.95 eV, which is about 0.2 eV higher than in water.[9] The reported oscillator strength is 0.69 for methanol, while the oscillator strength of the hydrated electron is 0.76.[9] With increasing pressure, the absorption maximum experiences a blueshift, which is more pronounced for the solvated electron in alcohols than for the hydrated electron.[9−11] For the temperature dependence of the absorption maximum, the opposite trend is observed.[12,13]

To investigate the solvation dynamics of electrons in alcohols, picosecond and femtosecond spectroscopy have been employed. The picosecond and femtosecond studies revealed that the solvation process consists of two steps, which were interpreted as the localization of the electron in a preexisting trap, followed by reorganization of the solvent molecules around the localized electron.[14,15] In more recent femtosecond pump−probe experiments on the equilibrated solvated electron in alcohols, the fastest process has been interpreted as the internal conversion to the electronic ground state, which is followed by a slower vibrational cooling process in the electronic ground state.[16]

Very recently, resonance Raman (RR) spectra of the solvated electron in water and alcohols have been obtained. Tauber and Mathies and Mizuno and Tahara independently measured the RR spectrum of the hydrated electron.[17−21] Tauber, Stuart, and Mathies also investigated the RR spectrum of the solvated electron in methanol, ethanol, and *n*-propanol.[22] For the solvated electron in methanol, RR spectra of different H/D substituted isotopomers of the solvent (CD_3OH, CH_3OD, and CD_3OD) have been obtained. It was found that for primary alcohols the OH stretching and bending modes are strongly enhanced in the RR spectra, as observed for the hydrated electron.[17−21] This finding shows that there are strong interactions between the excess electron and the OH groups in these solvents. Surprisingly, also significant enhancement of the CO stretching, CH_3 deformation, and in longer primary alcohols, of CC stretching vibrations has been observed.[22] For the solvated electron in methanol, the fingerprint lines of the RR spectrum are located at 475 cm^{-1}, 950−1020 cm^{-1}, ≈1330 cm^{-1}, ≈1440 cm^{-1}, and ≈3000 cm^{-1}.[21]

The generally accepted model for the description of the microscopic structure of the solvated electron in liquid water and alcohols is the so-called cavity model in which the electron is supposed to be localized within a cavity of the hydrogen-bonded network of the solvent molecules.[1−3,23] Computer simulations based on the cavity model have been shown to explain qualitatively the absorption spectrum[24] and the femtosecond spectroscopic experiments for methanol.[25−27] In these simulations, the electron has been treated quantum mechanically, whereas the solvent molecules have been treated classically, employing either a rigid or a flexible force-field model.[24−27] The electron−methanol interaction has been described by an empirical pseudopotential. In these simulations, the transitions from the s-type ground state to the three p-type excited states have been found to be mainly responsible for the optical absorption spectrum of the solvated electron. While the qualitative features of the absorption spectrum of the solvated electron

* To whom correspondence should be addressed. E-mail: Wolfgang.Domcke@ch.tum.de.
† Technical University of Munich.
‡ Polish Academy of Sciences.

10.1021/jp0574549 CCC: $33.50
Published on Web 04/05/2006

in methanol are reproduced, the width of the absorption profile is too small and the long tail of the spectrum toward the blue is lacking.[24]

Recently, Sobolewski and Domcke have proposed an alternative model for the solvated electron in water[28,29] which resembles earlier proposals of Robinson and collaborators.[30,31] It has been shown by restricted open-shell Hartree−Fock (ROHF) and density functional theory (DFT) calculations that the hydronium (H_3O) radical undergoes a spontaneous charge separation in an aqueous environment, resulting in a solvated hydronium cation (H_3O^+) and a solvated electron cloud. The hydronium−water clusters have been found to exhibit vertical excitation energies in the range of the absorption spectrum of the hydrated electron. It was concluded that hydronium water clusters can serve as finite-size model systems for the hydrated electron.[28] More recently, RR spectra of H_3OW_n ($W = H_2O$) clusters have been calculated.[32] The resulting simulated RR spectra are in reasonable agreement with the experimental RR spectra measured by Mizuno and Tahara as well as Tauber and Mathies.[17−21]

This cluster model of the solvated electron is extended to methanol in the present work. The analogue of the H_3O radical in water is the CH_3OH_2 hypervalent radical in methanol. We have investigated the absorption and RR spectra of $CH_3OH_2M_n$ clusters with $n = 1-3$. The ground-state structures and vibrational frequencies have been determined by DFT calculations. The electronic absorption and RR spectra of the clusters have been obtained by calculating the vertical excitation energies and their gradients with respect to normal modes, using time-dependent density functional theory (TDDFT).

2. Computational Methods

2.1. Calculation of RR Intensities. The RR intensities have been calculated within the time-dependent picture of the RR spectroscopy.[33,34] In the Born−Oppenheimer, short-time, and low-temperature approximations, the so-called Savin formula[35] gives the relative RR intensities.[33,34] For a single excited electronic state, the relative intensities of two fundamentals i and j are given by[35]

$$\frac{I^{(i)}}{I^{(j)}} = \frac{\kappa_i^2}{\kappa_j^2} \tag{1}$$

where κ_i and κ_j denote the gradients of the electronic excitation energy with respect to the dimensionless normal modes Q_i and Q_j in the electronic ground state.

If several electronic states are resonantly excited, then the RR amplitude of a given normal mode is the sum of the RR amplitudes of the individual excited electronic states. Since the dipole moments of different excited states are randomly oriented in complex systems without symmetry, the contributions of the interference terms to the RR intensities cancel to a large extent. The relative RR intensities are therefore given to a good approximation by the incoherent sum of the intensities of the excited states

$$I^{(i)} = \sum_k (f_k \kappa_i^{(k)})^2 \tag{2}$$

where f_k is the oscillator strength of the excited electronic state k and $\kappa_i^{(k)}$ is the corresponding energy gradient with respect to the normal coordinate Q_i.

2.2. Electronic-Structure Calculations. In previous studies of the hydrated hydronium radical, it has been found that frequencies and normal modes calculated by DFT and the Becke−Yang−Parr (B3LYP) functional[36−38] are in good agreement with those obtained by second-order Møller−Plesset perturbation theory (MP2). We therefore have optimized the geometries and calculated the frequencies and normal modes of the $CH_3OH_2M_n$ clusters by unrestricted DFT employing the B3LYP functional.[36−38] The B3LYP functional was used with the VWN5 exchange functional.[39] For all calculations, the 6-31+G** split valence double-ζ Gaussian basis set augmented with polarization functions on all atoms and diffuse functions on the heavy atoms[40] was used. This basis set has been extended by two additional diffuse sets of functions (one s function and one set of p functions) with an exponent of 0.02 [29] on the oxygen atoms. The GAUSSIAN 03 [41] package has been used in all calculations for the electronic ground state.

For the excited-state calculations, the TDDFT method has been employed. Vertical excitation energies, oscillator strengths, and the Cartesian gradients of the excited-state potential-energy surfaces (PESs) have been calculated at the TDDFT level using the TURBOMOLE program package,[42] which provides analytical gradients for excited states. The excited-state gradients with respect to dimensionless ground-state normal modes, $\kappa_j^{(k)}$, have been obtained as described previously.[32]

The minimum-energy path (MEP) and the barrier height for CH_3 elimination from the CH_3OH_2 radical have been investigated using MP2.

3. Results and Discussion

3.1. Geometries and Vibrational Frequencies. CH_3OH_2 is a Rydberg molecule analogous to H_3O. At the DFT/B3LYP level, the ground-state PES is barrierless with respect to dissociation into CH_3 and H_2O and therefore the ground-state geometry cannot be optimized. At the MP2 level, CH_3OH_2 exists as a local minimum of the ground-state PES, the geometry of which could be optimized. The barrier for the dissociation into CH_3 and H_2O is merely 1.48 kcal/mol and is the lowest barrier for dissociation. The PES of H_3O, for comparison, exhibits a barrier for the dissociation into H and H_2O of 3.37 kcal/mol at the same level of theory. CH_3OH_2 is thus less stable than H_3O with respect to the elimination of a water molecule.

Since the PES minimum corresponding to CH_3OH_2 is extremely shallow, the harmonic approximation is not applicable here. The calculation of vibrational energy levels and wave functions for multidimensional anharmonic PES is beyond the scope of the present work. We therefore have restricted the calculation of RR spectra to the $CH_3OH_2M_n$, $n = 1, 2, 3$, clusters, for which the harmonic approximation is applicable at least in a qualitative sense. The treatment of larger clusters ($n > 3$) is very demanding because the geometry optimizations and frequency calculations (calculation of the Hessian) become extremely tedious and time-consuming with growing cluster size. In particular, the floppy torsions of the CH_3 groups complicate the geometry optimizations.

The equilibrium structures of the $CH_3OH_2M_n$ clusters, $n = 1-3$, are shown in Figure 1as stick models together with the singly occupied molecular orbital (SOMO). CH_3OH_2 forms two strong hydrogen bonds in the $n = 2$ and $n = 3$ clusters, acting as the proton donor. As found previously for H_3OW_n,[28] the electron detaches from the CH_3OH_2 radical when the latter is solvated by methanol molecules. One observes a charge separation between the $CH_3OH_2^+$ core and the unpaired electron; see parts b and c of Figure 1. With growing cluster size, the distance between the cationic core and the electron increases until the electron can be regarded as detached from the $CH_3OH_2^+$ core.

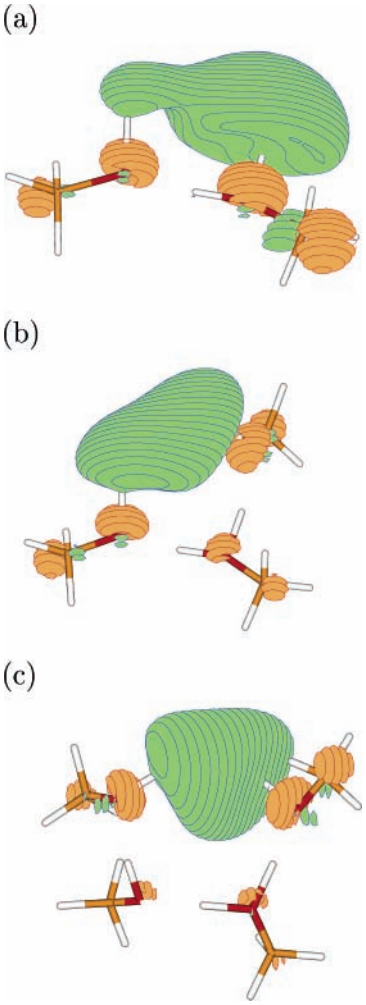

Figure 1. Equilibrium structures of the $CH_3OH_2M_n$ clusters. The singly occupied molecular orbital (SOMO) also is shown (electron density cut 0.04). Panel (a) shows the geometry and the SOMO for the cluster with $n = 1$, panel (b) for the cluster with $n = 2$, and panel (c) for the cluster with $n = 3$.

TABLE 1: Intermolecular Vibrational Frequencies (in cm^{-1}) of $CH_3OH_2M_n$ Clusters ($n = 1-3$), Calculated at the DFT/B3LYP(VWN5) Level

normal mode	CH_3OH_2M	$CH_3OH_2M_2$	$CH_3OH_2M_3$
inter	62.8	39.4	34.4
	92.7	73.8	53.3
	102.3	79.5	60.4
	133.3	91.4	75.8
	148.1	96.0	81.0
	263.1	112.0	90.5
		124.0	98.3
		130.3	99.2
		158.2	104.1
		169.7	109.0
		289.3	123.5
		385.0	126.9
			139.5
			158.8
			174.9
			228.0
			337.7
			409.3

The vibrational frequencies of intermolecular and intramolecular vibrations of the OH, HOH, and CH_3 groups are given in Tables 1−3. The intramolecular vibrations of methanol consist of the OH-related vibrations (OH in-plane bending, OH torsion, and OH stretching), the CO stretching vibration, and

TABLE 2: Vibrational Frequencies (in cm^{-1}) Related to the OH/HOH Groups of $CH_3OH_2M_n$ Clusters ($n = 1-3$), Calculated at the DFT/B3LYP(VWN5) Level[a]

normal mode	CH_3OH_2M	$CH_3OH_2M_2$	$CH_3OH_2M_3$
OH torsion	*427.6*	506.7	521.4
	604.6	564.7	548.6
			989.7
HOH torsion		**1209.9**	**1256.8**
CO stretching	**804.3**	932.3	*940.3*
	947.0	*970.6*	*1007.4*
	984.7	*999.1*	*1025.9*
OH in-plane bending	1063.5	1041.6	1031.6
	1310.3	1062.9	1057.4
	1349.7	1312.1	1109.2
		1355.4	*1128.5*
		1386.2	*1311.4*
		1401.1	*1357.5*
			1370.2
			1430.0
			1444.1
			1527.8
HOH bending	**1575.0**	**1740.4**	**1729.3**
HOH asymm. stretching	**1902.2**	**1811.0**	**1648.9**
HOH symm. stretching	**2457.2**	**2180.0**	**2078.6**
OH stretching	3468.3	3147.7	2859.1
		3178.1	2960.1
			3231.2

[a] Frequencies in normal font represent CH_3OH vibrations, bold ones represent CH_3OH_2 vibrations, and italic ones represent vibrations of mixed character.

TABLE 3: Vibrational Frequencies (in cm^{-1}) Related to the CH_3 Groups of $CH_3OH_2M_n$ Clusters ($n = 1-3$), Calculated at the DFT/B3LYP(VWN5) Level[a]

normal mode	CH_3OH_2M	$CH_3OH_2M_2$	$CH_3OH_2M_3$
CH_3 rocking	**1120.8**	**1130.0**	*1135.3*
	1158.6	**1153.1**	1157.9
	1170.2	1157.6	1166.7
		1166.1	**1169.8**
			1180.2
umbrella (symm. bending)	**1383.2**	*1433.0*	*1448.1*
	1448.6	1450.0	1456.9
	-	*1451.3*	1475.4
asymm. bending a''	**1473.2**	1487.0	1484.8
(CH_3 deformation)	1491.7	1487.2	1489.5
		1498.4	**1491.5**
asymm. bending a'	**1484.1**	**1490.8**	*1494.7*
(CH_3 deformation)	1501.8	1503.0	*1497.8*
		1503.6	1499.6
			1503.8
			1507.4
symm. stretching	3051.8	3043.1	3026.4
	3080.2	3045.2	3045.5
		3067.3	3048.2
			3061.7
asymm. stretching a''	3132.6	3126.8	3095.8
	3179.6	3127.0	3113.6
		3159.1	3126.1
			3172.4
asymm. stretching a'	3166.3	3160.6	3138.7
	3207.6	3161.4	3140.5
		3179.6	**3150.0**
			3159.8

[a] Frequencies in normal font represent CH_3OH vibrations, bold ones represent CH_3OH_2 vibrations, and italic ones represent vibrations of mixed character.

the CH_3-related vibrations (CH_3 rocking, CH_3 symmetric and asymmetric bending vibrations, and CH_3 symmetric and asymmetric stretching vibrations). Following the notation of ref 43, the labels a' and a'' in Table 3 refer to the symmetry of the CH_3 group itself. For the CH_3OH_2 part, there are the bending, the symmetric and asymmetric stretching vibrations of the H_2O

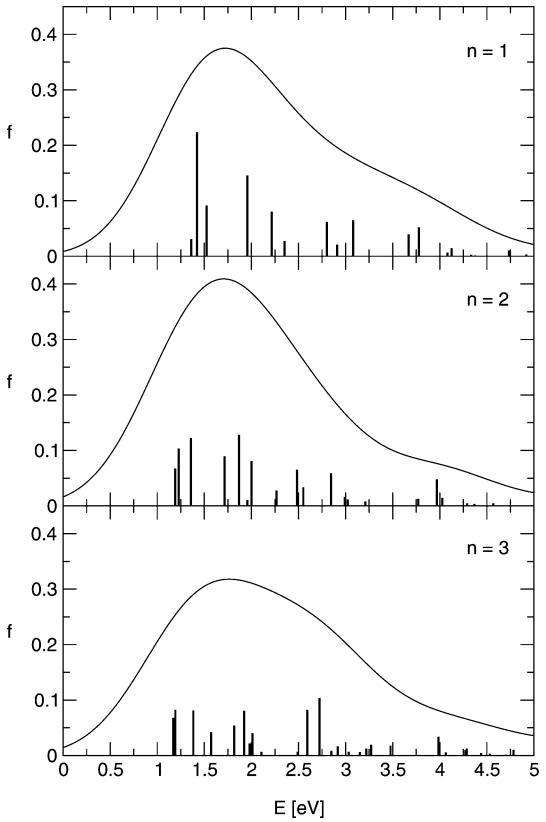

Figure 2. Vertical excitation spectrum of the $CH_3OH_2M_n$ clusters ($n = 1-3$), calculated at the TDDFT/B3LYP(VWN5) level and convoluted with a Gaussian function (fwhm = 1.3 eV).

group, the HOH torsion vibration, the OH in-plane-bending vibration, the CO stretching vibration, and the above-mentioned CH_3 vibrations. In the clusters, vibrations of different monomers can mix. In these mixings, not only vibrations of the same kind may be involved.

With growing cluster size, only the HOH-related vibrations and the OH stretching vibrations experience significant changes. The frequency of the HOH bending vibration of CH_3OH_2 shifts to the blue with growing cluster size. A redshift can be observed, on the contrary, for the frequencies of the HOH and OH stretching vibrations. Compared with gas-phase methanol,[43] the frequencies of the OH stretching vibrations in the clusters experience a strong redshift of up to 600 cm^{-1}, depending on the cluster size, as a result of hydrogen bonding and solvation of the unpaired electron. For the other vibrational frequencies, less pronounced changes relative to the frequencies of gas-phase methanol are found.

3.2. Absorption Spectra. The calculated vertical excitation spectra of the $CH_3OH_2M_n$, $n = 1-3$, clusters are shown as stick spectra in Figure 2. The height of the sticks represents the oscillator strength. The stick spectrum has been convoluted with a Gaussian broadening function (half width 1.3 eV), to account for Franck−Condon and thermal broadening effects. The resulting spectral envelopes are broad and asymmetric bands with maxima near 1.8 eV and integral oscillator strengths of about 0.88.

As shown in Figure 3, the absorption spectrum of the solvated electron in methanol is a broad, asymmetric and featureless band with a maximum at 1.95 eV (0 bar, 300 K) and an oscillator strength of 0.69.[9] The spectrum extends up to ≈4 eV, with the full width at half maximum (fwhm) being 1.37 eV.[9]

The convoluted spectrum of the largest cluster ($n = 3$) is a broad and asymmetric band with a maximum at 1.76 eV. The

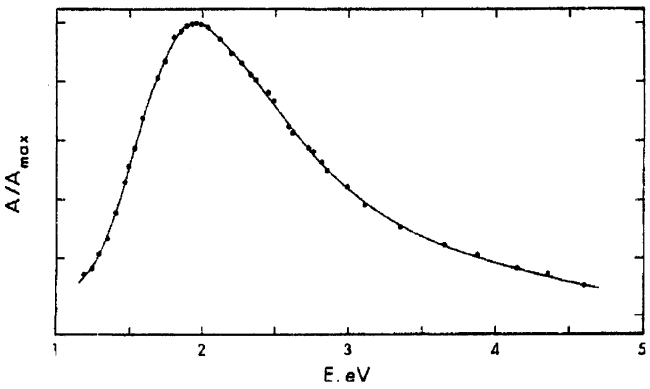

Figure 3. Experimental optical absorption spectrum of the solvated electron in methanol at 27 °C and 1 bar, adapted from ref 9.

width of the band is 2.4 eV. Compared with the experimental spectrum of the solvated electron in liquid methanol (see Figure 3), the maximum absorption is about 0.2 eV too low and the width is too large. The long tail to the blue, on the other hand, is well reproduced. That the absorption maximum of the clusters is lower than observed in liquid methanol is to be expected, since the solvated electron of the cluster model considered here is partially a surface-type electron (see Figure 1). Full enclosure of the electron in larger clusters will lead to a contraction of the electronic charge distribution (due to the strong hydrogen-bond network in methanol) and thus a blueshift of the electronic absorption spectrum.

The molecular dynamics simulations based on the cavity model of the solvated electron in methanol have predicted that only the transitions to the three lowest *p* states carry significant intensity.[25,26] The absorption maximum is underestimated by about 0.2 eV, and the calculated fwhm of 1.07 eV is significantly smaller than the measured width.[26] It seems that only three intensity carrying excited states cannot account for the optical absorption spectrum of the solvated electron, especially not for its extended tail to higher energies.

It should be emphasized that the spectra in Figure 2 are not simulated absorption spectra of thermal clusters. The convolution of all electronic transitions with a single Gaussian broadening function clearly is an oversimplification. The important and qualitatively new aspect is the fact that the TDDFT calculations for the cluster model predict a multitude of electronic transitions with significant oscillator strengths between 1 and 4 eV, in marked contrast to the molecular dynamics calculations based on the cavity model. The absorption spectra of the cluster model clearly exhibit more chemical complexity than those obtained by the cavity model.

3.3. Resonance Raman Intensities. For the calculation of the RR intensities of the $CH_3OH_2M_n$ clusters, all excited states in the range 1−4 eV have been included that possess at least 5% of the oscillator strength of the experimental absorption spectrum of the solvated electron in methanol. The RR intensities have been calculated from eq 2 for all vibrational modes of the clusters.

The resulting RR intensities are given in the Supporting Information (Tables 1−3). The simulated RR spectra are shown in Figure 4. The upper panel of Figure 4 shows the simulated RR spectrum of CH_3OH_2M, the middle panel that of $CH_3OH_2M_2$, and the lowest panel that of $CH_3OH_2M_3$. The simulated spectra have been convoluted with Gaussian broadening functions with a fwhm of 180 cm^{-1} for frequencies smaller than 2000 cm^{-1} and 571 cm^{-1} for frequencies larger than 2000 cm^{-1}. These line widths account in a qualitative manner for anharmonic couplings and thermal broadening effects.

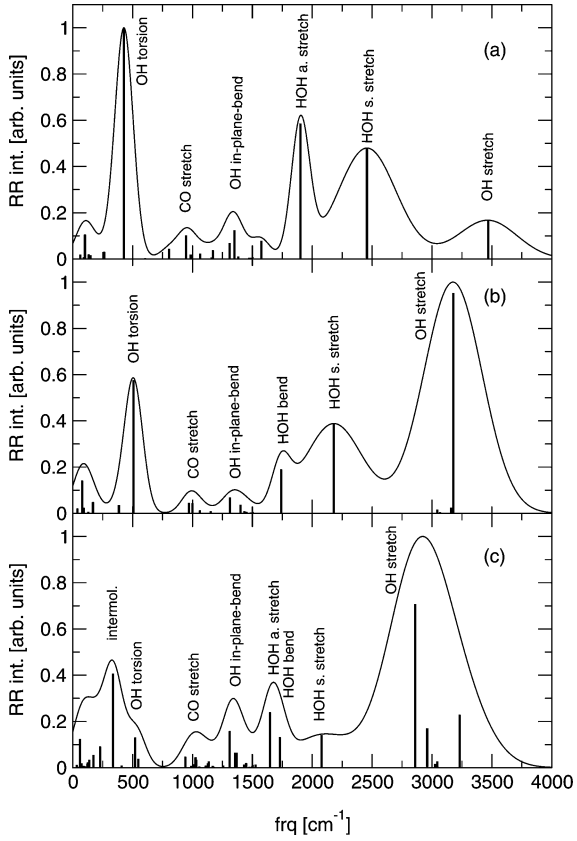

Figure 4. Simulated RR spectra of the $CH_3OH_2M_n$ clusters, with (a) $n = 1$, (b) $n = 2$, and (c) $n = 3$ obtained from vibrational frequencies and RR intensities calculated at the DFT/B3LYP(VWN5) level, convoluted with a Gaussian broadening function (fwhm = 180 cm^{-1} for frequencies up to 2000 cm^{-1} and fwhm = 571 cm^{-1} for frequencies from 2000 to 4000 cm^{-1}).

In the simulated RR spectrum of CH_3OH_2M (Figure 4a), enhanced intensities can be observed for the OH torsion, the CO stretching, the OH in-plane bending, the HOH bending, the HOH asymmetric, and symmetric stretching vibrations. The OH stretch intensity is comparatively low.

Figure 4b shows the simulated RR spectrum of the $n = 2$ cluster. In this case, the OH stretching vibration is strongly enhanced and the dominant line in the spectrum. In the frequency range of about 750 to 1800 cm^{-1}, there are three peaks which arise mainly from the CO stretching, the OH in-plane-bending, and the HOH bending vibrations.

The simulated RR spectrum of $CH_3OH_2M_3$ is shown in Figure 4c. Here, a peak at about 400 cm^{-1} has gained considerable intensity. It arises primarily from an intermolecular vibrational mode and to a lesser extent from an OH torsion mode. In the spectra of the smaller clusters, this low-energy peak arises from the OH torsion mode only. The following three peaks in the range of about 750 to 1800 cm^{-1} are related to CO stretching, OH in-plane-bending, and HOH asymmetric stretching and bending vibrations. The HOH symmetric stretching vibration at about 2000 cm^{-1} is less intense than that in the smaller clusters. It can be expected that this peak vanishes for larger clusters. The OH stretching vibration shows up as a broad and intense peak at about 3000 cm^{-1}.

The experimental RR spectrum of Tauber et al.[22] for the solvated electron in methanol is shown in Figure 5. The lowest-energy peak at about 500 cm^{-1} has been assigned to the OH torsion vibration.[22] In the frequency range between 800 and 1800 cm^{-1}, there are three peaks with comparable intensity. These three peaks have been assigned as the CO stretching, the OH in-plane-bending, and the CH_3 deformation vibration.[22] The broad and intense peak at about 3000 cm^{-1} clearly corresponds to the OH stretching vibration. All of the OH-related vibrations in the experimental RR spectrum of the solvated electron in methanol exhibit a significant downshift in frequency relative to liquid methanol[43] which indicates that the OH groups are strongly interacting with the excess electron.

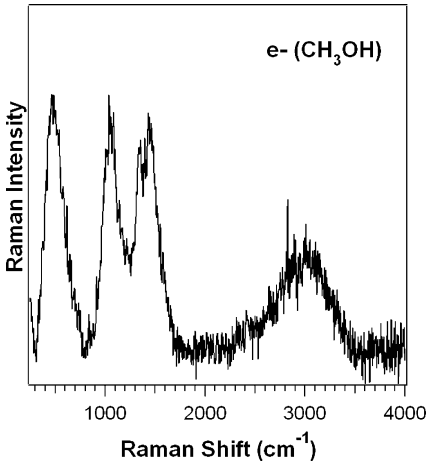

Figure 5. Experimental RR spectrum of the solvated electron in liquid methanol (with the friendly permission of R. Mathies).

The simulated spectrum of the CH_3OH_2M cluster shows clear deviations from the experimental spectrum. In particular, the symmetric HOH stretching mode, which is strongly enhanced in Figure 4a, is not present in the experimental spectrum. Nevertheless, important features of the observed RR spectrum like the enhanced OH torsion vibration at 427 cm^{-1} and the OH stretching mode are already present.

The simulated RR spectrum of the $n = 2$ cluster (Figure 4b) shows improved agreement with the experimental spectrum. However, the intensities of the peaks in the range of 800−1800 cm^{-1} are too low relative to the OH torsion and OH stretch. Moreover, the HOH symmetric stretch appears as a strong peak near 2000 cm^{-1}, in a region where the experimental spectrum (Figure 5) shows little intensity.

The simulated RR spectrum of $CH_3OH_2M_3$ (Figure 4c) is in rather good agreement with the experimental RR spectrum, although the assignments of the peaks are partially different. According to the cluster model, the lowest-energy peak at about 500 cm^{-1} arises primarily from an intermolecular mode rather than from the OH torsion mode.

According to the cluster model calculations, the peak at about 1650 cm^{-1} arises mainly from the HOH asymmetric stretching and to a lesser extent from the HOH bending mode. Comparing the vibrational frequencies of the HOH asymmetric stretching vibration for the investigated clusters, one observes that the frequency decreases with growing cluster size and tends toward 1500 cm^{-1}. The cluster model calculations do not confirm the assignment of the peak at 1500 cm^{-1} in ref 22 as CH_3 deformation. CH_3-related vibrations show very little intensity enhancement in the calculated spectra. The peak assigned as the CH_3 deformation vibration in liquid methanol[22] is not reproduced by the calculations, which seems to be a limitation of the cluster model. To clarify this discrepancy between the cluster model and the experiment for liquid methanol, the treatment of larger clusters seems to be necessary.

When the intensities of Figure 4c are compared with the experimental RR spectrum, there are some differences. The peaks at about 500, 1000, 1400, and 1650 cm^{-1}, which show

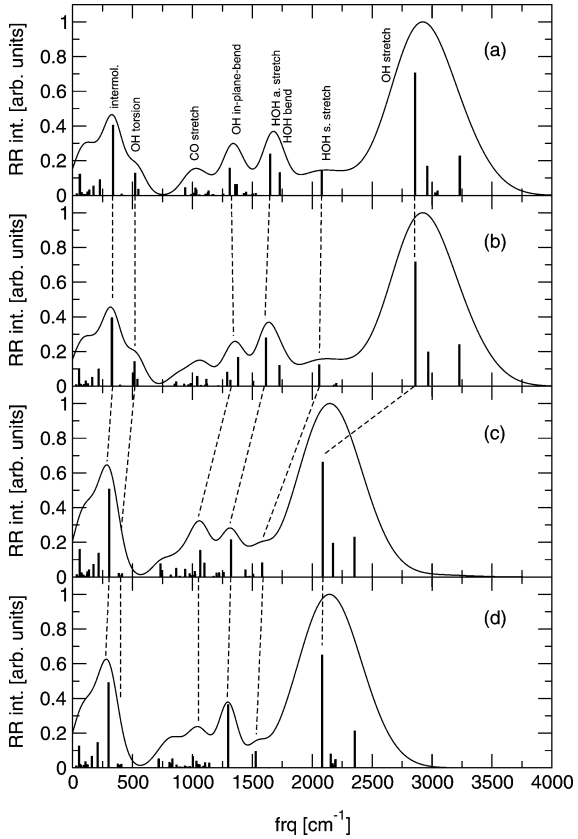

Figure 6. Simulated RR spectra of $CH_3OH_2M_3$ for different isotopes: (a) $CH_3OH_2(CH_3OH)_3$, (b) $CD_3OH_2(CD_3OH)_3$, (c) $CH_3OD_2(CH_3OD)_3$, and (d) $CD_3OD_2(CD_3OD)_3$ obtained from vibrational frequencies and RR intensities calculated at the DFT/B3LYP(VWN5) level, convoluted with a Gaussian broadening function (fwhm = 180 cm^{-1} for frequencies up to 2000 cm^{-1} and fwhm = 571 cm^{-1} for frequencies from 2000 to 4000 cm^{-1}).

almost equal intensities in the experimental RR spectrum, appear with different intensities in the simulated RR spectrum of the $n = 3$ cluster. It can be noticed, however, that with growing cluster size the intensities of these four peaks become more equal.

In Figure 6, the simulated RR spectra of H/D substituted isotopomers of the $CH_3OH_2M_3$ cluster are shown. Panel (a) shows the spectrum of the unsubstituted cluster for comparison. In panel (b), the simulated RR spectrum of the CD_3-substituted cluster is given. The RR spectrum of this isotopomer is almost identical with that of the unsubstituted cluster. This shows that the vibrations of the CH_3 group are not enhanced in the RR spectrum of $CH_3OH_2M_3$. The peak at about 1000 cm^{-1} now arises from several different modes (HOH/OH torsion, CH_3 deformation, CO stretching, and OH in-plane-bending modes) rather than from the CO stretching mode alone. Panel (c) shows the simulated RR spectrum of the OD substituted cluster. As expected, the OH stretching vibrations exhibit a significant redshift. The OH torsion vibration loses intensity. In this case, the peak at about 750 cm^{-1} cannot be assigned as the CO stretch vibration, since several different vibrations contribute to this peak. The simulated RR spectrum of the fully deuterated cluster is shown in panel (d). It is rather similar to the OD substituted one, which again indicates the insignificance of the RR activity of CH_3 vibrations.

Figure 7 shows the experimental RR spectra of the solvated electron in correspondingly H/D substituted methanol with the assignments suggested by Tauber et al.[22] The spectra exhibit the expected pronounced redshift of the OH stretch vibrations in CH_3OD and CD_3OD. The intense peak at 500 cm^{-1} in CH_3-

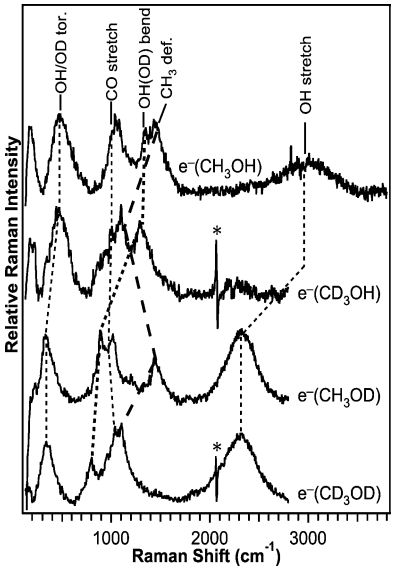

Figure 7. Experimental RR spectrum of the solvated electron in liquid methanol with different H/D isotope substitutions (with the friendly permission of R. Mathies).

OH exhibits an isotope shift of about 150 cm^{-1}, in agreement with the assignment as OH torsion by Tauber et al. This indicates that this peak indeed is mainly of OH torsion character as found in the present work for the $n = 1$ and $n = 2$ clusters.

The correlations of the lowest-energy peak, the peak of the OH(OD) in-plane-bending and of the OH(OD) stretching mode with respect to different isotopomers, are similar in the experimental and the cluster spectra. The peak which is assigned as the CO stretching vibration is unaffected by H/D substitution in both spectra, as expected. The only essential difference in the assignments between the cluster spectra (Figure 6) and the experimental spectra (Figure 7) concerns the CH_3 deformation mode, which does not show up with significant intensity in the calculated spectra. The reason for this could lie in the limited size of the calculated clusters.

4. Conclusions

The geometric and electronic structures, vibrational frequencies, and normal modes of $CH_3OH_2M_n$ clusters, $n = 1-3$, have been investigated by DFT/B3LYP calculations. It has been shown that with growing cluster size a charge separation process takes place. The orbital of the unpaired electron detaches from the $CH_3OH_2^+$ cation, resulting in a localized electron cloud at the opposite end of the cluster.

The vertical excitation spectrum of the clusters has been obtained by TDDFT/B3LYP calculations. The calculations predict a multitude of electronic transitions in the energy range from 1 to 4 eV with an integrated oscillator strength of about 0.88. The envelope obtained by convolution of the calculated stick spectrum with a Gaussian function of 1.3 eV fwhm is peaked near 1.8 eV and exhibits a long tail extending to higher energies. This latter feature is a characteristic signature of the absorption spectrum of the solvated electron in methanol which could not be reproduced by the existing simulations within the cavity model.[24]

The RR intensities of the normal modes of the $CH_3OH_2M_n$ clusters have been estimated via a generalization of the Savin formula[35] for multiple excited electronic states. The simulated RR spectrum of the largest cluster, $CH_3OH_2M_3$, is in good qualitative agreement with the experimental RR spectrum of the solvated electron in methanol.[22] The simulations within the

cluster model reveal that the observed peaks in the RR spectrum arise from several normal-mode excitations; the assignment of the RR peaks in terms of normal modes can therefore be of only qualitative character.

The H/D isotope effects in the RR spectrum reported by Tauber et al.[22] have been investigated within the $CH_3OH_2M_n$ cluster model. The pronounced redshift of the OH stretching mode upon deuteration is reproduced. The assignment of correlations of the three peaks in the range of 800−1500 cm^{-1} has been found to be ambiguous owing to the multiple character of these peaks. The intense low-energy peak (400−500 cm^{-1}) has been assigned as a superposition of OH torsion and intermolecular modes. From the experiment, it seems clear that this peak arises from the OH torsion vibration alone.[22] As the CH_3-related vibrations are not enhanced in the cluster spectra, the isotope shift of the CH_3 deformation vibration could not be observed in the simulated spectra. This may be a consequence of the limited cluster sizes treated here.

We conclude that $CH_3OH_2M_n$ clusters can be considered as useful finite-size model systems for the computation of the spectroscopic properties of the solvated electron in methanol, although the treatment of larger clusters would be desirable for a more substantiated comparison with the experimental results for the solvated electron in methanol. It is likely that this conclusion also holds for the solvated electron in higher alcohols such as ethanol or propanol, which show similar experimental RR spectra as the solvated electron in methanol.[22]

Acknowledgment. Support for this work has been obtained from the Deutsche Forschungsgemeinschaft and the Fonds der Chemischen Industrie. Generous allocation of computing time by the Leibniz Rechenzentrum is acknowledged.

Supporting Information Available: Tables showing the relative RR intensities of intermolecular vibrations in $CH_3OH_2M_n$ clusters, of intramolecular OH/HOH-related vibrations in $CH_3OH_2M_n$ clusters, and of CH_3-related vibrations in $CH_3OH_2M_n$ clusters. This material is available free of charge via the Internet at http://pubs.acs.org.

References and Notes

(1) Gould, R. F., Ed. *Solvated Electron*; Advances in Chemistry; American Chemical Society Washington, DC, 1965.
(2) Schindewolf, U. *Angew. Chem., Int. Ed. Engl.* **1978**, *17*, 887.
(3) Feng, D.-F.; Kevan, L. *Chem. Rev.* **1980**, *80*, 1.
(4) Tuttle, T. R., Jr.; Golden, S. *J. Phys. Chem.* **1991**, *95*, 5725.
(5) Taub, I. A.; Harter, D. A.; Sauer, M. C.; Dorfman, L. M. *J. Chem. Phys.* **1964**, *41*, 979.
(6) Sauer, M. C.; Arai, S.; Dorfman, L. M. *J. Chem. Phys.* **1965**, *42*, 708.
(7) Jha, K. N.; Freeman, G. R. *J. Chem. Phys.* **1968**, *48*, 5480.
(8) Shiraishi, H.; Ishigure, K.; Morokuma, K. *J. Chem. Phys.* **1988**, *88*, 4637.
(9) Jou, F.-Y.; Freeman, G. R. *J. Phys. Chem.* **1977**, *81*, 909.
(10) Jou, F.-Y.; Freeman, G. R. *J. Phys. Chem.* **1979**, *83*, 261.
(11) Robinson, M. G.; Jha, K. N.; Freeman, G. R. *J. Chem. Phys.* **1971**, *55*, 4933.
(12) Arai, S.; M. C. Sauer, J. *J. Chem. Phys.* **1966**, *44*, 2297.
(13) K. N. Jha, G. L. B.; Freeman, G. R. *J. Chem. Phys.* **1972**, *76*, 3876.
(14) Kenney-Wallace, G. A.; Jonah, C. D. *J. Phys. Chem.* **1982**, *86*, 2572.
(15) Shi, X.; Long, F. H.; Lu, H.; Eisenthal, K. B. *J. Phys. Chem.* **1995**, *99*, 6917.
(16) Walhout, P. K.; Alfano, J. C.; Kimura, Y.; Silva, C.; Reid, P. J.; Barbara, P. F. *Chem. Phys. Lett.* **1995**, *232*, 135.
(17) Mizuno, M.; Tahara, T. *J. Phys. Chem. A* **2001**, *105*, 8823.
(18) Mizuno, M.; Tahara, T. *J. Phys. Chem. A* **2003**, *107*, 2411.
(19) Tauber, M.; Mathies, R. *J. Phys. Chem. A* **2001**, *105*, 10952.
(20) Tauber, M. J.; Mathies, R. A. *Chem. Phys. Lett.* **2002**, *354*, 518.
(21) Tauber, M.; Mathies, R. *J. Am. Chem. Soc.* **2003**, *125*, 1394.
(22) Tauber, M.; Stuart, C. M.; Mathies, R. *J. Am. Chem. Soc.* **2004**, *126*, 3414.
(23) Ogg, R. A. *J. Am. Chem. Soc.* **1946**, *68*, 155.
(24) Turi, L.; Mosyak, A.; Rossky, P. J. *J. Chem. Phys.* **1997**, *107*, 1970.
(25) Mosyak, A. A.; Prezhdo, O. V.; Rossky, P. J. *J. Chem. Phys.* **1998**, *109*, 6390.
(26) Mináry, P.; Turi, L.; Rossky, P. J. *J. Chem. Phys.* **1999**, *110*, 10953.
(27) Mosyak, A. A.; Prezhdo, O. V.; Rossky, P. J. *J. Mol. Struct.* **1999**, *485*−*486*, 545.
(28) Sobolewski, A. L.; Domcke, W. *Phys. Chem. Chem. Phys.* **2002**, *4*, 4.
(29) Sobolewski, A. L.; Domcke, W. *J. Phys. Chem. A* **2002**, *106*, 4158.
(30) Robinson, G. W.; Thistlewaite, P. J.; Lee, J. *J. Phys. Chem.* **1986**, *90*, 4224.
(31) Hameka, H. F.; Robinson, G. W.; Marsden, C. *J. Phys. Chem.* **1987**, *91*, 3150.
(32) Neumann, S.; Eisfeld, W.; Sobolewski, A.; Domcke, W. *Phys. Chem. Chem. Phys.* **2004**, *6*, 5297.
(33) Lee, S.-Y.; Heller, E. J. *J. Chem. Phys.* **1979**, *71*.
(34) Heller, E. J. *Acc. Chem. Res.* **1981**, *14*, 368.
(35) Savin, F. *Opt. Spectrosc.* **1965**, *19*, 555.
(36) Becke, A. D. *Phys. Rev. A* **1988**, *38*, 3098.
(37) Lee, C.; Yang, W.; Parr, R. G. *Phys. Rev. B* **1988**, *37*, 785.
(38) Becke, A. D. *J. Chem. Phys.* **1993**, *98*, 5648.
(39) Vosko, S.; Wilk, L.; Nussair, M. *Can. J. Phys.* **1980**, *58*, 1200.
(40) W. J. Hehre, R. D.; Pople, J. *J. Chem. Phys.* **1972**, *56*, 2257.
(41) Frisch, M. J.; Trucks, G. W.; Schlegel, H. B.; Scuseria, G. E.; Robb, M. A.; Cheeseman, J. R.; Montgomery, J. A., Jr.; Vreven, T.; Kudin, K. N.; Burant, J. C.; Millam, J. M.; Iyengar, S. S.; Tomasi, J.; Barone, V.; Mennucci, B.; Cossi, M.; Scalmani, G.; Rega, N.; Petersson, G. A.; Nakatsuji, H.; Hada, M.; Ehara, M.; Toyota, K.; Fukuda, R.; Hasegawa, J.; Ishida, M.; Nakajima, T.; Honda, Y.; Kitao, O.; Nakai, H.; Klene, M.; Li, X.; Knox, J. E.; Hratchian, H. P.; Cross, J. B.; Bakken, V.; Adamo, C.; Jaramillo, J.; Gomperts, R.; Stratmann, R. E.; Yazyev, O.; Austin, A. J.; Cammi, R.; Pomelli, C.; Ochterski, J. W.; Ayala, P. Y.; Morokuma, K.; Voth, G. A.; Salvador, P.; Dannenberg, J. J.; Zakrzewski, V. G.; Dapprich, S.; Daniels, A. D.; Strain, M. C.; Farkas, O.; Malick, D. K.; Rabuck, A. D.; Raghavachari, K.; Foresman, J. B.; Ortiz, J. V.; Cui, Q.; Baboul, A. G.; Clifford, S.; Cioslowski, J.; Stefanov, B. B.; Liu, G.; Liashenko, A.; Piskorz, P.; Komaromi, I.; Martin, R. L.; Fox, D. J.; Keith, T.; Al-Laham, M. A.; Peng, C. Y.; Nanayakkara, A.; Challacombe, M.; Gill, P. M. W.; Johnson, B.; Chen, W.; Wong, M. W.; Gonzalez, C.; Pople, J. A. *GAUSSIAN 03*, revision B.04; Gaussian Inc.: Pittsburgh, PA, 2003.
(42) Ahlrichs, R.; Bär, M.; Häser, M.; Horn, H.; Kölmel, C. *Chem. Phys. Lett.* **1989**, *162*, 165.
(43) Falk, M.; Whalley, E. *J. Chem. Phys.* **1961**, *34*, 1554.